Spin-Orbit Interactions in Ultrafast Molecular Processes

Francesco Talotta, Sabine Morisset, Nathalie Rougeau, D. Lauvergnat, Federica Agostini

Spin-orbit interactions in ultrafast molecular processes

Francesco Talotta *,[1,2] Sabine Morisset,[2] Nathalie Rougeau,[2] David Lauvergnat,[1] and Federica Agostini †[1]

[1]*Laboratoire de Chimie Physique, UMR 8000 CNRS/University Paris-Sud, University Paris-Saclay, 91405 Orsay, France*
[2]*Institut de Sciences Moléculaires d'Orsay, UMR 8214 CNRS/University Paris-Sud, University Paris-Saclay, 91405 Orsay, France*

We investigate spin-orbit interactions in ultrafast molecular processes employing the exact factorization of the electron-nuclear wavefunction. We revisit the original derivation by including spin-orbit coupling, and show how the dynamics driven by the time-dependent potential energy surface alleviates inconsistencies arising from different electronic representations. We propose a novel trajectory-based scheme to simulate spin-forbidden non-radiative processes, and we show its performance in the treatment of excited-state dynamics where spin-orbit effects couple different spin multiplets.

PACS numbers:

Spin-orbit (SO) interactions are responsible for fascinating phenomena that often have direct implications for technological advances. SO coupling makes it possible to tune magnetic properties of materials with light [1, 2], whereas the interaction between electronic charge and spin is exploited in the field of spintronics [3, 4] and molecular spintronics [5]; in organic light-emitting diodes SO effects allow to harness both singlet and triplet excitations for achieving high efficiency [6, 7]; the possibility of controlling spins in molecular assemblies has even found its way towards quantum information [8, 9]. Assessing a priori the importance of SO coupling is difficult. Being a relativistic effect, it is essential in describing *intersystem crossings* (ISCs) in systems with heavy transition metals [10–15]. ISC denotes a spin-forbidden non-radiative electronic transition between states of different spin multiplicity, to be distinguished from the ubiquitous internal conversion (IC) that takes place between states of the same spin multiplicity. Nonetheless, ISCs have been observed in processes involving light-element species [16–24], thus proving that the strength of SO interactions depends on the molecular geometry. Therefore, a theory that is able of treating IC and ISC on equal footing, without an a priori knowledge of the relative importance of the two effects, is highly desirable, especially for the study of (photo-induced) ultrafast dynamics in complex molecular systems.

The most common strategy to simulate ISC is to adapt molecular-dynamics schemes designed for IC: quantum wavepackets propagation techniques and trajectory-based approaches become, thus, readily available. Wavepacket propagation [16, 21, 25, 26] requires to precompute electronic potentials as functions of nuclear configurations, whereas trajectories evolve under the effect of forces [27–32] determined based on on-the-fly electronic-structure calculations – for this reason are suited to access complex systems. Nowadays, a widely-used technique for the treatment of IC/ISC is trajectory surface hopping [33, 34]. For IC, classical trajectories evolve "on" electronic potential energy surfaces, and hop from one surface to another to mimic an electronic transition preserving spin multiplicity. The extension of surface hopping to ISC has been proposed by different authors about a decade ago [28–31]. However, its use in this context remains still *highly debated*, concerning the choice of the most appropriate electronic representation to be used [35], *physically problematic*, exhibiting issues in preserving rotational invariance of the coupling with states in the same multiplet [35, 36], and *subject to inconsistencies*, in the use of different hopping rules for IC and ISC [28]. An intriguing and timely question thus arises, as to whether IC and ISC can be described within the same trajectory-based approach without incurring in the above-mentioned issues.

In the present Letter, we positively answer this question by employing the exact factorization (EF) of the electron-nuclear wavefunction [37, 38], and we show how IC/ISC can be addressed, in a consistent way, within the same theoretical construction. The EF will be formulated accounting for relativistic SO interactions in the time-dependent Schrödinger equation (TDSE), and a numerical procedure for trajectory-based on-the-fly calculations will be derived to simulate ultrafast IC/ISC processes. EF implies a very simple decomposition of the interacting electron-nuclear quantum-mechanical problem, that has led to profound physical insights into electronic and nuclear interactions underlying excited-state processes in the non-relativistic limit [37–47]. Here, our goal is to initiate a new chapter for the EF, and to demonstrate how such theoretical construction can be employed for numerical simulations including important effects due to SO interactions.

We consider the Hamitonian $\hat{H}(\boldsymbol{x},\boldsymbol{R}) = \hat{T}_n(\boldsymbol{R}) + \hat{H}_{BO}(\boldsymbol{x},\boldsymbol{R}) + \hat{H}_{SO}(\boldsymbol{x},\boldsymbol{R})$, with $\boldsymbol{x} = \boldsymbol{r},\boldsymbol{s}$ indicating N_{el} electronic positions and spins, and $\boldsymbol{R}$ N_n nuclear positions. $\hat{T}_n(\boldsymbol{R})$ is the nuclear kinetic energy, $\hat{H}_{BO}(\boldsymbol{x},\boldsymbol{R})$ the Born-Oppenheimer (BO) Hamiltonian, containing the electronic kinetic energy and the position-dependent interactions, $\hat{H}_{SO}(\boldsymbol{x},\boldsymbol{R})$ the SO interaction [28, 48, 49]. The solution of the TDSE $i\hbar\partial_t\Psi(\boldsymbol{x},\boldsymbol{R},t) = \hat{H}(\boldsymbol{x},\boldsymbol{R})\Psi(\boldsymbol{x},\boldsymbol{R},t)$ can be exactly factored as $\Psi(\boldsymbol{x},\boldsymbol{R},t) = \Phi_{\boldsymbol{R}}(\boldsymbol{x},t)\chi(\boldsymbol{R},t)$, with $\chi(\boldsymbol{R},t)$ the

nuclear wavefunction, and $\Phi_{\boldsymbol{R}}(\boldsymbol{x},t)$ the electronic conditional factor. Coupled electronic and nuclear equations,

$$i\hbar\partial_t\Phi_{\boldsymbol{R}} = \left[\hat{H}_{BO} + \hat{H}_{SO} + \hat{U}_{en}[\Phi_{\boldsymbol{R}},\chi] - \epsilon(\boldsymbol{R},t)\right]\Phi_{\boldsymbol{R}} \quad (1)$$

$$i\hbar\partial_t\chi = \left[\sum_{\nu=1}^{N_n}\frac{[-i\hbar\nabla_\nu + \boldsymbol{A}_\nu(\boldsymbol{R},t)]^2}{2M_\nu} + \epsilon(\boldsymbol{R},t)\right]\chi, \quad (2)$$

can be derived under the condition $\int d\boldsymbol{x}|\Phi_{\boldsymbol{R}}(\boldsymbol{x},t)|^2 = 1\ \forall\,\boldsymbol{R},t$. The integration over the variable $\boldsymbol{x}$ stands for an integration over $\boldsymbol{r}$ and a sum over $\boldsymbol{s}$. The time-dependent vector potential, $\boldsymbol{A}_\nu(\boldsymbol{R},t) = \langle\Phi_{\boldsymbol{R}}(t)| - i\hbar\nabla_\nu\Phi_{\boldsymbol{R}}(t)\rangle_{\boldsymbol{x}}$, and the electron-nuclear coupling operator, $\hat{U}_{en} = \sum_\nu[-i\hbar\nabla_\nu - \boldsymbol{A}_\nu]^2/(2M_\nu) + (-i\hbar\nabla_\nu\chi/\chi + \boldsymbol{A}_\nu)\cdot(-i\hbar\nabla_\nu - \boldsymbol{A}_\nu)/M_\nu$, are defined as in the original derivation [50]. We have used here the index ν to label N_n nuclei, and the symbol $\langle\cdot\rangle_{\boldsymbol{x}}$ to indicate the integration over $\boldsymbol{x}$. In this formulation of EF, the expression of the time-dependent potential energy surface (TDPES) contains the SO interaction: $\epsilon(\boldsymbol{R},t) = \langle\Phi_{\boldsymbol{R}}(t)|\hat{H}_{BO} + \hat{H}_{SO} + \hat{U}_{en} - i\hbar\partial_t|\Phi_{\boldsymbol{R}}(t)\rangle_{\boldsymbol{x}}$. Under a $(\boldsymbol{R},t)$-dependent phase transformation of the electronic and nuclear wavefunctions, the EF product remains unchanged, but the potentials transform as standard gauge potentials [50, 51]. In particular, the TDPES can be decomposed as the sum of a gauge-invariant (GI) and gauge-dependent (GD) contributions, namely $\epsilon_{GI}(\boldsymbol{R},t) = \langle\Phi_{\boldsymbol{R}}(t)|\hat{H}_{BO} + \hat{H}_{SO} + \hat{U}_{en}|\Phi_{\boldsymbol{R}}(t)\rangle_{\boldsymbol{x}}$ and $\epsilon_{GD}(\boldsymbol{R},t) = \langle\Phi_{\boldsymbol{R}}(t)| - i\hbar\partial_t|\Phi_{\boldsymbol{R}}(t)\rangle_{\boldsymbol{x}}$.

This formulation of EF with SO coupling, while formally similar to the original derivation of non-relativistic EF, is able to clearly indicate the route towards a consistent trajectory-based approach to IC/ISC.

Let us first answer the question: *What is the appropriate electronic representation to describe ISC, and what forces are to be used to propagate classical trajectories?* Usually, two "viewpoints" are proposed in the literature: spin-diabatic and spin-adiabatic. The spin-diabatic (sd) basis is the set of eigenstates of $\hat{H}_{BO}$,

$$\hat{H}_{BO}(\boldsymbol{x},\boldsymbol{R})\varphi_{\boldsymbol{R}}^{(J,M_{S_J})}(\boldsymbol{x}) = \epsilon_{sd}^{(J,M_{S_J})}(\boldsymbol{R})\varphi_{\boldsymbol{R}}^{(J,M_{S_J})}(\boldsymbol{x}), \quad (3)$$

which are also eigenstates of $\hat{S}^2, \hat{S}_z$ (with eigenvalues $\hbar^2 S_J(S_J+1)$ and $\hbar M_{S_J}$). The index J labels the multiplets, each including $2S_J+1$ states, and $\epsilon_{sd}^{(J,M_{S_J})}(\boldsymbol{R})$ indicates the energy eigenvalue. The spin-adiabatic (sa) representation is defined as

$$\left[\hat{H}_{BO}(\boldsymbol{x},\boldsymbol{R}) + \hat{H}_{SO}(\boldsymbol{x},\boldsymbol{R})\right]\varphi_{\boldsymbol{R}}^{(j)}(\boldsymbol{x}) = \epsilon_{sa}^{(j)}(\boldsymbol{R})\varphi_{\boldsymbol{R}}^{(j)}(\boldsymbol{x}), \quad (4)$$

where $\epsilon_{sa}^{(j)}(\boldsymbol{R})$ indicates the energy eigenvalue corresponding to state j. The spin-diabatic basis is often preferred for interpreting spectroscopic results, since states can be labelled depending on their spins, e.g., singlets, or triplets; the spin-adiabatic states are, instead, combinations of different spin multiplicities. In an approximate trajectory-based treatment of the dynamics, using one or the other representation is not always equivalent [28, 32, 34].

To analyze this point further, we introduce a model Hamiltonian [65] describing the interaction of a singlet (S) with a triplet (T) in 1D nuclear space [35],

$$\hat{H} = \hat{T}_n(R) + \begin{pmatrix} E_S(R) & z(R) & ib(R) & z^*(R) \\ z^*(R) & E_T(R) & 0 & 0 \\ -ib(R) & 0 & E_T(R) & 0 \\ z(R) & 0 & 0 & E_T(R) \end{pmatrix}. \quad (5)$$

The details of the model are given in the Supporting Information (Section SI.1). The electronic matrix is given in the spin-diabatic basis, with diagonal elements $\langle\varphi_{\boldsymbol{R}}^{(J,M_{S_J})}|\hat{H}_{BO}|\varphi_{\boldsymbol{R}}^{(J,M_{S_J})}\rangle$, and off-diagonal elements $\langle\varphi_{\boldsymbol{R}}^{(J,M_{S_J})}|\hat{H}_{SO}|\varphi_{\boldsymbol{R}}^{(K,M_{S_K})}\rangle$.

If trajectory-based calculations are performed in the spin-diabatic basis, *(i)* the forces are computed from the diagonal elements of the electronic matrix in Eq. (5), and *(ii)* the coupling among electronic states is mediated by the nuclear kinetic energy and by the SO coupling. The kinetic coupling is often called nonadiabatic, and is responsible for IC. Nonadiabatic and SO couplings might be of very different nature, the former spatially localized in regions of nuclear configuration space where electronic states are close in energy or degenerate, the latter extremely delocalized (see Section SI.1 of the Supporting Information). For this reason, the algorithms designed for IC usually cannot be directly applied to ISC and need to be revisited [27, 28, 30, 32, 35].

If calculations are performed in the spin-adiabatic basis, SO interactions do not explicitly appear in the problem, since *(i)* classical forces are determined from the energy eigenvalues of $\hat{H}_{BO} + \hat{H}_{SO}$, and *(ii)* the coupling among the states becomes fully kinetic. In this case, IC and ISC can be treated fully consistently within the same schemes. Apart from preventing the labelling of the spin states for interpretation purposes, using a spin-adiabatic representation presents a practical drawback: quantum-chemistry codes widely used for on-the-fly dynamics do not provide efficient ways for computing gradients of the SO coupling (that are needed for the forces) [30, 52], unless simplifications in the electronic-structure theory are invoked [53].

With the EF, instead: *(i)* classical forces that drive nuclear dynamics are determined from the time-dependent vector potential and TDPES of Eq. (2) [51, 54–61], whose expressions are invariant if different representations are used, i.e., either spin-adiabatic or spin-diabatic; *(ii)* the coupling among electronic states is fully accounted for by $\hat{H}_{BO}+\hat{H}_{SO}$ and by the electron-nuclear coupling operator $\hat{U}_{en}$ of Eq. (1). To illustrate how ISCs

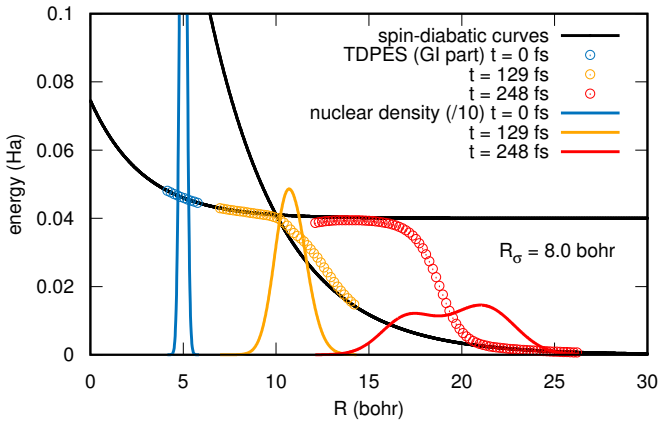

FIG. 1: Singlet and triplet energy curves (black lines) compared with $\epsilon_{GI}(R,t)$ at $t = 0, 129, 248$ fs (colored dots). The nuclear densities – divided by 10 – at the same times are shown as colored lines. $R_\sigma = 8.0$ bohr is the position where the SO coupling changes sign.

are treated within the EF, we compute the exact TDPES for the model Hamiltonian (5), by initializing the dynamics in the singlet state, as described in the Supporting Information (Section SI.2). The gauge is set by imposing that the vector potential potential is identically zero [51]. Figure 1 shows three snapshots along the dynamics of $\epsilon_{GI}(R,t)$ (colored dots), superimposed to the spin-diabatic curves (black lines). The nuclear densities at the corresponding times are shown as well (colored lines). We recall here that the GI part of the TDPES is the only term containing SO interaction. In Fig. 1 it is clear that $\epsilon_{GI}(R,t)$ adapts its shape along the dynamics, and in particular in the region where $E_S(R)$ and $E_T(R)$ cross, the TDPES slightly follows the (spin-diabatic) shape of the singlet before smoothly switching to the triplet. For completeness, we mention that $\epsilon_{GD}(R,t)$ is either constant or piecewise constant as function of R, such that it does not alter the slope of $\epsilon_{GI}(R,t)$ and it only reduces the height of its step [51, 62, 63].

A second question naturally arises at this point: *Is it possible to employ the EF to derive a practical trajectory-based scheme to simulate ISCs?* A coupled-trajectory mixed quantum-classical (CT-MQC) algorithm [64] has been derived previously from Eqs. (1) and (2), and applied to describe ultrafast IC in molecules [55, 56, 58]. As the approximations of the original CT-MQC rely on the adiabatic representation, the extension of this method to the inclusion of SO effects in the spin-adiabatic basis is straightforward. However and as mentioned earlier, electronic-structure methods usually provide quantities in the spin-diabatic representation. Capitalizing on the representation-free nature of the EF quantities, we show here that CT-MQC can be used in any representation by expressing it also in a spin-diabatic basis. Therefore, we show in the following that, within the EF formalism, IC and ISC can be treated fully consistently even in the approximate, trajectory-based formulation. The gauge freedom allows us to avoid calculation of gradients of the SO Hamiltonian.

A classical limit performed on the nuclear equation (2) allows us to define the force used to propagate the trajectories employing the TDPES, with inclusion of SO coupling, and the time-dependent vector potential. If $\boldsymbol{P}_\nu^{(\alpha)}(t)$ denotes the momentum of the nucleus ν along the trajectory α at time t, the expression of the force is

$$\dot{\boldsymbol{P}}_\nu^{(\alpha)}(t) = \boldsymbol{F}_{\nu,\mathrm{Eh}}^{(\alpha)}(t) + \boldsymbol{F}_{\nu,\mathrm{deco}}^{(\alpha)}(t) + \boldsymbol{F}_{\nu,\mathrm{SO}}^{(\alpha)}(t). \tag{6}$$

The first two terms on the right-hand side are the same as in CT-MQC, namely a mean-field-like term – indicated as "Ehrenfest" (Eh) – and a term accounting for quantum decoherence – labelled "deco" [42]. The additional term accounts for SO interactions, and its expression will be given below. The electronic wavefunction $\Phi_{\boldsymbol{R}}(\boldsymbol{x},t)$ is expanded in the spin-diabatic basis of Eq. (3), and we indicate with the symbol $C_{J,M_{S_J}}(\boldsymbol{R},t)$ the expansion coefficients. Evolution equations for the coefficients can be derived from Eq. (1). When the classical limit is performed, the dependence on $\boldsymbol{R}$ is transformed into a dependence on the trajectory α, such that

$$\dot{C}_{J,M_{S_J}}^{(\alpha)}(t) = \dot{C}_{J,M_{S_J},\mathrm{Eh}}^{(\alpha)}(t) + \dot{C}_{J,M_{S_J},\mathrm{deco}}^{(\alpha)}(t) + \dot{C}_{J,M_{S_J},\mathrm{SO}}^{(\alpha)}(t). \tag{7}$$

As in Eq. (6) the mean-field-like and the quantum-decoherence terms are the same as in the original derivation of CT-MQC. SO effects are accounted for in the additional term.

The detailed procedure yielding the SO terms in Eqs. (6) and (7) follows the same steps as for the non-relativistic terms of the original CT-MQC (see Refs. [42, 58, 60]). Those additional terms are

$$\boldsymbol{F}_{\nu,\mathrm{SO}}^{(\alpha)}(t) = \frac{2}{\hbar}\sum_{J,K}\sum_{M_{S_J},M_{S_K}} \boldsymbol{f}_{\nu,JM_{S_J}}^{(\alpha)}(t) \times \mathrm{Im}\left[H_{SO,JK,M_{S_J}M_{S_K}}^{(\alpha)}(t) C_{J,M_{S_J}}^{(\alpha)*}(t) C_{K,M_{S_K}}^{(\alpha)}(t)\right] \tag{8}$$

$$\dot{C}_{J,M_{S_J},\mathrm{SO}}^{(\alpha)}(t) = -\frac{i}{\hbar}\sum_{K,M_{S_K}} H_{SO,JK,M_{S_J}M_{S_K}}^{(\alpha)}(t) C_{K,M_{S_K}}^{(\alpha)}(t), \tag{9}$$

with $\boldsymbol{f}_{\nu,JM_{S_J}}^{(\alpha)}(t) = \int^t -\nabla_\nu \epsilon_{sd}^{(J,M_{S_J}),(\alpha)} d\tau$ the (spin-diabatic) force accumulated along the trajectory α. Eqs. (6) and (7) have been derived by imposing that the scalar potential in the nuclear equation is fully absorbed into the vector potential [60].

We test the new algorithm on the model system defined in Eq. (5). The TDSE has been solved exactly to

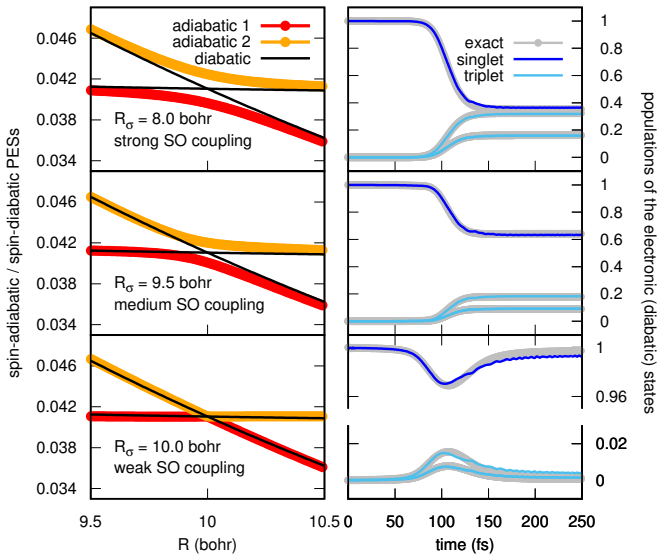

FIG. 2: Left: Singlet and triplet potential curves (black lines) compared to the spin-adiabatic curves (colored lines) for different strengths of the SO coupling. Right: Exact (gray lines) and CT-MQC-SO (colored lines) populations of the singlet (blue) and triplet (light-blue) states.

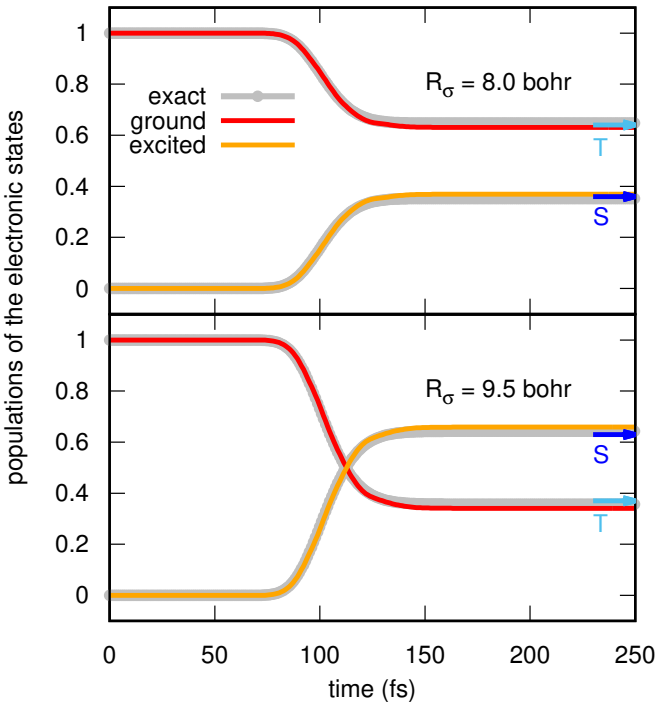

FIG. 3: Spin-adiabatic populations from exact (gray) and CT-MQC-SO (red and orange) calculations for two values of R_σ. Final populations of the singlet (S, blue) and triplet (T, cyan) states are indicated by the arrows.

provide benchmark data for the trajectory-based solution. To demonstrate the robustness of the new algorithm, the time trace of electronic populations is shown in Fig. 2 (right panels) for different strengths of the SO interaction (left panels). The agreement between exact (gray lines) and trajectory-based (blue, singlet, and light-blue, triplets, lines) results is remarkable in all regimes. As it is clear from Fig. 2 the components of the triplet can be treated separately in the new scheme, which we will refer to as CT-MQC-SO, and it is not necessary to introduce *ad hoc* schemes to estimate a "group" SO coupling [31, 35, 36] as in surface hopping.

Note that, due to the delocalized nature of the SO coupling, Eqs. (8) and (9) can only go to zero via a decoherence process, namely if a given trajectory "collapses" to a single electronic state at long times. In this case, the coefficient corresponding to that state becomes unity, while all others are zero. Therefore, the quantum-decoherence terms in Eqs. (6) and (7), signature of a coupled-trajectory scheme such as CT-MQC-SO [60], are essential to avoid spurious population transfers.

The final point to be addressed relates to the question: *Is the dynamics generated based on CT-MQC-SO really consistent for IC and ISC?* As we have stated previously, the treatment of IC and ISC is really consistent *only* in the spin-adiabatic basis, because kinetic and SO couplings are treated in the same way. To prove consistency within CT-MQC-SO, we will compare results of the trajectory-based calculations in the spin-adiabatic and spin-diabatic basis. To this end, we introduce the transformation presented in Ref. [35], and we reduce the 4-states Hamiltonian of Eq. (5) to a 2-states problem

$$\hat{H} = \hat{T}_n(R) + \begin{pmatrix} E_S(R) & \alpha(R) \\ \alpha(R) & E_T(R) \end{pmatrix}, \tag{10}$$

whose details are given in the Supporting Information (Section SI.1). We solve exactly the TDSE and we compute the populations of the two spin-adiabatic states. They are compared to the trajectory-based results in Fig. 3 [66]. Together, Fig. 2 and 3 show perfect agreement between exact and CT-MQC-SO results in both spin-diabatic and spin-adiabatic basis, and thus consistency between propagation in the two representations. For completeness, and since in the asymptotic $t \to +\infty$ region spin-diabatic and spin-adiabatic states are the same, we indicate with an arrow the final populations of the singlet/triplet states in Fig. 3.

To investigate further the differences between CT-MQC-SO in the two representations for the model Hamiltonian (10), we compare in Fig. 4 the spatial distributions of trajectories at $t = 0, 129, 248$ fs, and we compute the value of the GI part of the TDPES at the position of each trajectory. As reference, we also show the exact value of the TDPES. In the simulation performed in the spin-adiabatic representation (colored dots), the shape of $\epsilon_{GI}(R,t)$ (purple lines) is closely reproduced. By contrast, the trajectories evolving in the spin-diabatic representation (gray dots) seem to evolve slightly faster

in comparison to the spin-adiabatic trajectories. The reason for this discrepancy is twofold: *(i)* the approximations underlying CT-MQC-SO, in particular the neglect of spatial derivatives of the expansion coefficients $C_{J,M_{S_J}}(\boldsymbol{R},t)$, and *(ii)* the difficulty in accurately capturing oscillating terms of the TDPES when the spin-diabatic basis is employed (see Section SI.3 of the Supporting Information). Figure 3 proves that CT-MQC-SO is robust, for instance, to predict electronic populations, but not all observables might be estimated with the same level of accuracy as shown in Fig. 4.

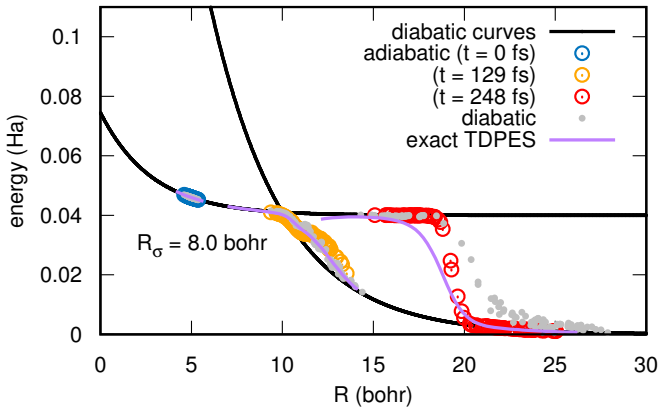

FIG. 4: Singlet and triplet potential curves (black lines) compared with the exact $\epsilon_{GI}(R,t)$ (purple lines) and with $\epsilon_{GI}^{(\alpha)}(t)$ calculated at the positions of the trajectories (dots) at $t = 0, 129, 248$ fs. Colored dots refer to spin-adiabatic results, and gray dots to spin-diabatic results.

It is worth stressing again, that EF is a representation-free formulation of the TDSE, thus the quantum-classical limit performed on Eqs. (1) and (2) is representation-independent. The actual implementation of the quantum-classical equations, i.e., the "quantum-classical algorithm", relies on combinations of electronic-structure information that depend on the representation. In CT-MQC-SO, we succeeded in computing TDPES and time-dependent vector potential without altering the original algorithm. This feature is a strength, especially since we showed that nuclear dynamics in different representations are very similar. However, discrepancies might be encountered, and only systematic studies under different conditions might provide information of general validity.

To conclue, in this work we have proposed an exact-factorization formulation of the quantum-mechanical electron-nuclear problem including spin-orbit interactions. The aim is to be able to address ultrafast intersystem crossings by employing the theoretical framework previously develop to investigate internal conversions. Starting with the exact factorization, we have briefly described the procedure leading to a trajectory-based algorithm readily suitable for on-the-fly molecular dynamics. We have applied the algorithm, dubbed CT-MQC-SO, to simulate the dynamics in a 1D model system representing interacting singlet and triplet states. Comparisons between CT-MQC-SO and exact dynamics have highlighted the extremely good performance of the new algorithm in both the spin-adiabatic and spin-diabatic representations.

The authors would like to thank Hugo Bessone, Lea-Maria Ibele, and Emanuele Marsili for their help in developing the code to compute the TDPES for the 4-state model, and E-CAM for its financial support in this development. F. A. acknowledges funding for equipment received from the Department of Chemistry of the University Paris-Saclay. This work is supported by a public grant from the "Laboratoire d'Excellence Physics Atoms Light Mater" (LabEx PALM) overseen by the French National Research Agency (ANR) as part of the "Investissements d'Avenir" program (reference: ANR-10-LABX-0039-PALM).

* francesco.talotta@u-psud.fr
† federica.agostini@u-psud.fr

[1] V. Shokeen, M. S. Piaia, J.-Y. Bigot, T. Müller, P. Elliott, J. Dewhurst, S. Sharma, and E. Gross, Phys. Rev. Lett. **119**, 107203 (2017).
[2] P. Elliott, T. Müller, J. K. Dewhurst, S. Sharma, and E. K. U. Gross, Scientific Reports **6**, 38911 (2016).
[3] A. Soumyanarayanan, N. Reyren, A. Fert, and C. Panagopoulos, Nature **539**, 509 (2016).
[4] F. Hellman and *et al.*, Rev. Mod. Phys. **89**, 025006 (2017).
[5] D. Sun, E. Ehrenfreund, and Z. V. Vardeny, Chem. Comm. **50**, 1781 (2014).
[6] H. Noda, H. Nakanotani, and C. Adachi, Sci. Adv. **4**, eaao6910 (2018).
[7] P. K. Samanta, D. Kim, V. Coropceanu, and J.-L. Brédas, J. Am. Chem. Soc. **139**, 4042 (2017).
[8] B. K. Rugg, B. T. Phelan, N. E. Horwitz, R. M. Young, M. D. Krzyaniak, M. A. Ratner, and M. R. Wasielewski, J. Am. Chem. Soc. **139**, 15660 (2017).
[9] Y. Wu, J. Zhou, J. N. Nelson, R. M. Young, M. D. Krzyaniak, and M. R. Wasielewski, J. Am. Chem. Soc. **140**, 13011 (2018).
[10] I. Tavernelli, B. F. E. Curchod, and U. Rothlisberger, Chem. Phys. **391**, 101 (2011).
[11] H. Ando, S. Iuchi, and H. Sato, Chem. Phys. Lett. **535**, 177 (2012).
[12] H. Brahim and C. Daniel, Comput. Theo. Chem. **1040-1041**, 219 (2014).
[13] M. Chergui, Dalton Trans. **41**, 13022 (2012).
[14] R. M. van der Veen, A. Cannizzo, F. van Mourik, A. V. Jr., and M. Chergui, J. Am. Chem. Soc. **133**, 305 (2010).
[15] A. Cannizzo, A. M. Blanco-Rodríguez, A. E. Nahha, J. Šebera, S. Záliš, A. V. Jr., and M. Chergui, J. Am. Chem. Soc. **130**, 8967 (2008).
[16] D. S. N. Parker, R. S. Minns, T. J. Penfold, G. A. Worth, and H. H. Fielding, Chem. Phys. Lett. **469**, 43 (2009).
[17] B. Han and Y. Zheng, J. Comput. Chem. **32**, 3520 (2011).

[18] S. Mai, P. Marquetand, and L. González, J. Chem. Phys. **140**, 204302 (2014).
[19] K. Rajak and B. Maiti, J. Chem. Phys. **133**, 011101 (2010).
[20] B. Fu, Y.-C. Han, J. M. Bowman, L. Angelucci, N. Balucani, F. Leonori, and P. Casavecchia, Proc. Natl. Acad. Sci. **109**, 9733 (2012).
[21] R. S. Minns, D. S. N. Parker, T. J. Penfold, G. A. Worth, and H. H. Fielding, Phys. Chem. Chem. Phys. **12**, 15607 (2010).
[22] H. Li, A. Kamasah, S. Matsika, and A. G. Suits, Nature Chem. **11**, 123 (2019).
[23] L. Martínez-Fernández, I. Corral, G. Granucci, and M. Persico, Chem. Sci. **5**, 1336 (2014).
[24] M. Richter, P. Marquetand, J. González-Vázquez, I. Sola, and L. González, J. Phys. Chem. Lett. **3**, 3090 (2012).
[25] T. J. Penfold, E. Gindensperger, C. Daniel, and C. M. Marian, Chem. Rev. **118**, 6975 (2018).
[26] G. Capano, M. Chergui, U. Rothlisberger, I. Tavernelli, and T. J. Penfold, J. Phys. Chem. A **118**, 9861 (2014).
[27] B. F. E. Curchod, C. Rauer, P. Marquetand, L. González, and T. J. Martínez, J. Chem. Phys. **144**, 101102 (2016).
[28] F. F. de Carvalho and I. Tavernelli, J. Chem. Phys. **143**, 224105 (2015).
[29] G. Cui and W. Thiel, J. Chem. Phys. **141**, 124101 (2014).
[30] M. Richter, P. Marquetand, J. González-Vázquez, I. Solab, and L. González, J. Chem. Theory Comput. **7**, 1253 (2011).
[31] W. Hu, G. Lendvay, B. Maiti, and G. C. Schatz, J. Phys. Chem. A **112**, 2093 (2008).
[32] R. Valero and D. G. Truhlar, J. Phys. Chem. A **111**, 8536 (2007).
[33] P. Marquetand, M. Richter, J. González-Vázquez, I. Sola, and L. González, Faraday Discuss. **153**, 261 (2011).
[34] S. Mai, P. Marquetand, and L. González, Int. J. Quant. Chem. **115**, 1215 (2015).
[35] G. Granucci, M. Persico, and G. Spighi, J. Chem. Phys. **137**, 22A501 (2012).
[36] B. Fu, B. C. Shepler, and J. M. Bowman, J. Am. Chem. Soc. **133**, 7957 (2011).
[37] A. Abedi, N. T. Maitra, and E. K. U. Gross, Phys. Rev. Lett. **105**, 123002 (2010).
[38] F. Agostini and B. F. E. Curchod, WIREs Comput. Mol. Sci. **9**, e1417 (2019).
[39] A. Abedi, F. Agostini, Y. Suzuki, and E. K. U. Gross, Phys. Rev. Lett **110**, 263001 (2013).
[40] S. K. Min, A. Abedi, K. S. Kim, and E. K. U. Gross, Phys. Rev. Lett. **113**, 263004 (2014).
[41] E. Khosravi, A. Abedi, and N. T. Maitra, Phys. Rev. Lett. **115**, 263002 (2015).
[42] S. K. Min, F. Agostini, and E. K. U. Gross, Phys. Rev. Lett. **115**, 073001 (2015).
[43] R. Requist and E. K. U. Gross, Phys. Rev. Lett. **117**, 193001 (2016).
[44] A. Schild and E. K. U. Gross, Phys. Rev. Lett. **118**, 163202 (2017).
[45] A. Scherrer, F. Agostini, D. Sebastiani, E. K. U. Gross, and R. Vuilleumier, Phys. Rev. X **7**, 031035 (2017).
[46] B. F. E. Curchod and F. Agostini, J. Phys. Chem. Lett. **8**, 831 (2017).
[47] L. Lacombe, N. M. Hoffmann, and N. T. Maitra, arXiv:1906.02651v1 [physics.chem-ph] (2019).
[48] E. van Lenthe, E. J. Baerends, and J. G. Snijders, J. Chem. Phys. **99**, 4597 (1993).
[49] C. M. Marian, WIREs Comput. Mol. Sci. **2**, 187 (2012).
[50] A. Abedi, N. T. Maitra, and E. K. U. Gross, J. Chem. Phys. **137**, 22A530 (2012).
[51] F. Agostini, A. Abedi, Y. Suzuki, S. K. Min, N. T. Maitra, and E. K. U. Gross, J. Chem. Phys. **142**, 084303 (2015).
[52] F. F. de Carvalho, B. F. E. Curchod, T. J. Penfold, and I. Tavernelli, J. Chem. Phys. **140**, 144103 (2014).
[53] G. Granucci and M. Persico, J. Comput. Chem. **32**, 2690 (2011).
[54] G. Gossel, F. Agostini, and N. T. Maitra, J. Chem. Theory Comput. **14**, 4513 (2018).
[55] B. F. E. Curchod, F. Agostini, and I. Tavernelli, Euro. Phys. J. B **91**, 168 (2018).
[56] F. Agostini, B. F. E. Curchod, R. Vuilleumier, I. Tavernelli, and E. K. U. Gross, in *Handbook of Materials Modeling*, edited by W. Andreoni and S. Yip (Springer Netherlands, 2018), pp. 1–47.
[57] F. Agostini, I. Tavernelli, and G. Ciccotti, Euro. Phys. J. B **91**, 139 (2018).
[58] S. K. Min, F. Agostini, I. Tavernelli, and E. K. U. Gross, J. Phys. Chem. Lett. **8**, 3048 (2017).
[59] J.-K. Ha, I. S. Lee, and S. K. Min, J. Phys. Chem. Lett. **9**, 1097 (2018).
[60] F. Agostini, S. K. Min, A. Abedi, and E. K. U. Gross, J. Chem. Theory Comput. **12**, 2127 (2016).
[61] Y. Suzuki, A. Abedi, N. T. Maitra, and E. K. U. Gross, Phys. Chem. Chem. Phys. **17**, 29271 (2015).
[62] B. F. E. Curchod, F. Agostini, and E. K. U. Gross, J. Chem. Phys. **145**, 034103 (2016).
[63] F. Agostini and B. F. E. Curchod, Euro. Phys. J. B **91**, 141 (2018).
[64] F. Agostini, S. K. Min, I. Tavernelli, and G. H. Gossel, *CTMQC*, `https://e-cam.readthedocs.io/en/latest/Quantum-Dynamics-Modules/modules/CTMQC/readme.html` (2018).
[65] The model can exemplify singlet-triplet coupling in molecules such as formaldehyde or acetone under displacement of the oxygen atom in the direction perpendicular to the place formed by the CO group and the atoms directly linked to it.
[66] Note that trajectory-based results for $R_\sigma = 10.0$ bohr have not be presented because in the spin-adiabatic basis the two states are degenerate at $R = R_\sigma$. This yields an infinitely localized singular coupling that is numerically challenging to capture when computing the nonadiabatic couplings.